Investigation of the glass formation region and optical properties of the phases obtained in the As$_2$S$_3$–CdSe system

I.I.Aliyev[1], C.A.Ahmedova[2], N.N.Mursakulov[3], N.N.Abdulzade[3], I.I.Abbasov[4], A.L.Bakhtiyarov[4], Kh.M.Gashimov[5]

[1] M.Nagiyev Institute of Catalysis and Inorganic Chemistry, Azerbaijan National Academy of Sciences
[2] Adiyaman State University Faculty of Arts and Sciences, Department of Chemistry, Turkey
[3] Institute of Physics, National Academy of Sciences of Azerbaijan
[4] Azerbaijan State Oil and Industry University
[5] Azerbaijan State University of Economics

The As$_2$S$_3$–CdSe system was studied using differential thermal, X-ray diffraction, microstructure analyses, as well as microhardness and density measurements, and a phase diagram was constructed. It was established that a new Cd$_3$As$_2$S$_3$Se$_3$ compound is formed in the system which crystallizes in the rhombic syngony with the unit cell parameters: $a = 0.618$; $b = 1,424$; $c = 0.782$ nm, $Z = 3$, $\rho_{pycn.} = 4.95 \cdot 10^3$ kg/m^3; $\rho_{X\text{-}ray} = 5.04 \cdot 10^3$ kg/m^3. In the As$_2$S$_3$–CdSe system, the boundaries of the glass region formed on the basis of As$_2$S$_3$ were determined. It was revealed that in the mode of slow cooling, the glass formation region on the basis of As$_2$S$_3$ extends to 15 mol. % CdSe, and in the quenching mode in air, it is 20 mol. % CdSe. For the Cd$_3$As$_2$S$_3$Se$_3$ compound, the spectral distribution of the photocurrent is investigated as a function of the wavelength. The temperature dependence of the electrical conductivity of glassy alloys with 5, 10, 15, 20 and 25 mol.% CdSe was investigated in the temperature range of 290–450 K. A nanostructured thin film of Cd$_3$As$_2$S$_3$Se$_3$ compound was obtained by vacuum deposition, and optical properties were studied. When adding low-resistance alloys with 5, 10, 15, 20 and 25 mol. % CdSe in the composition of the high-resistance compound As$_2$S$_3$, the electrical conductivity of the alloys increases depending on the composition and temperature.

Keywords: system, chalcogenides, phase diagram, semiconductors, solidus.

Дослідження області склоутворення та оптичних властивостей фаз, отриманих у системі As$_2$S$_3$–CdSe. *І.І.Алієв, С.А.Ахмедова, Н.Н.Мурсакулов, Н.Н.Абдулзаде, І.І.Аббасов, А.Л.Бахтіяров, Х.М.Гашимов*

Вивчено систему As$_2$S$_3$–CdSe за допомогою диференціально-термічного, рентгенодифракційного, мікроструктурного аналізів, вимірювання мікротвердості та щільності; побудовано фазову діаграму. Встановлено, що у системі утворюється нова сполука Cd$_3$As$_2$S$_3$Se$_3$, яка кристалізується у ромбічній сингонії з параметрами елементарної комірки: $a = 0,618$; $b = 1424$; $c = 0,782$ нм, $Z = 3$, $\rho_{пікн.} = 4,95 \cdot 10^3$ кг/м^3; $\rho_{рент} = 5,04 \cdot 10^3$ кг/м^3. У системі As$_2$S$_3$–CdSe на основі As$_2$S$_3$ визначено межі областей склоформування. Виявлено, що у режимі повільного охолодження область склоформування на основі As$_2$S$_3$ простягається до 15 мол. % CdSe, а у режимі закалювання у повітрі складає 20 мол. % CdSe. Для сполуки Cd$_3$As$_2$S$_3$Se$_3$ вивчено спектральне розподілення фотоструму за довжиною хвилі. Досліджено температурну залежність електропровідності склоподібних сплавів з 5, 10, 15, 20 і 25 мол. % CdSe в інтервалі температур 290–450 К.

Наноструктуровану тонку плівку сполуки $Cd_3As_2S_3Se_3$ отримано методом вакуумного осадження і досліджено оптичні властивості. При додаванні низькоомних сплавів 5, 10, 15, 20 та 25 мол. % CdSe до складу високоомної сполуки As_2S_3, електропровідність сплавів збільшується в залежності від складу та температури.

Изучена система As_2S_3–CdSe с помощью дифференциального термического, рентгенодифракционного, микроструктурного анализов, измерения микротвердости и плотности, построена фазовая диаграмма. Установлено, что в системе образуется новое соединение $Cd_3As_2S_3Se_3$, которое кристаллизуется в ромбической сингонии с параметрами элементарной ячейки: $a = 0,618$; $b = 1,424$; $c = 0,782$ нм, $Z = 3$, $\rho_{пикн.} = 4,95 \cdot 10^3$ кг/м^3; $\rho_{рент.} = 5,04 \cdot 10^3$ кг/м^3. В системе As_2S_3–CdSe на основе As_2S_3 определены границы области стеклообразования. Выявлено, что в режиме медленного охлаждения область стеклообразования на основе As_2S_3 простирается до 15 мол. % CdSe, в режиме закалки на воздухе составляет 20 мол. % CdSe. Для соединения $Cd_3As_2S_3Se_3$ изучено спектральное распределение фототока по длинам волн. Температурная зависимость электропроводности стеклообразных сплавов 5, 10, 15, 20 и 25 мол. % CdSe исследована в интервале температур 290–450 К. Наноструктурированная тонкая пленка соединения $Cd_3As_2S_3Se_3$ получена методом вакуумного напыления, исследованы её оптические свойства. При добавлении низкоомных сплавов 5, 10, 15, 20 и 25 мол. % CdSe в состав высокоомного соединения As_2S_3, электропроводность сплавов увеличивается в зависимости от состава и температуры.

1. Introduction

Chalcogenides of subgroup II, elements of Zn and Cd, as well as multicomponent phases based on them are widely used in optical systems as photosensitive semiconductor material [1–4].

It is known that arsenic chalcogenides and their alloys are IR-transparent and are widely used in optical information processing systems [5–9], in particular, in elements of acousto-optic devices [10–14] and targets for video codes [15–21]. Therefore, the search for new vitreous semiconductors based on As_2S_3 and As_2Se_3 is a relevant and interesting topic, both in theory and in practice.

The important physicochemical parameters and fields of application of glassy alloys obtained in the As_2S_3–CdSe system have been investigated. Previously, we have investigated some quasi-binary sections of the quaternary As–Cd–S–Se system [22–24].

The aim of this work was to study the chemical interaction and glass formation in the As_2S_3–CdSe system, as well as photoelectric and electrophysical properties of new semiconducting phases and glassy alloys.

2. Experimental

The alloys of the As_2S_3–CdSe system were synthesized from a mixture of As_2S_3 and CdSe components melted at temperatures from 773 K to 1273 K in quartz ampoules evacuated to a pressure of 0.133 Pa. The cooling rate varied from 303 K/h to 333 K/h. The physicochemical analysis of the As_2Se_3–CdSe alloys was carried out both in the glassy and in the crystalline states. The interactions in the As_2S_3–CdSe system were studied in the concentration range 0–100 mol. % CdSe.

The phase diagram was constructed from the data of differential thermal analysis (DTA), X-ray powder diffraction (XRD), microstructure analysis (MSA), as well as microhardness and density measurements.

Temperature curves were recorded using a Thermoscan-2 low-frequency temperature recorder at a heating rate of 283 K/min. Temperature measurements of phase transformations were carried out using combined chromel-alumel thermocouples. Heating and cooling of the alloys were carried out in tubular resistance electric furnaces.

Thermograms were recorded under vacuum. The alloys were heated and annealed in Stepanov's fired quartz vessels which were placed in the hole of the steel block. Al_2O_3 was used as a reference.

X-ray powder diffraction patterns were recorded on a D2 PHASER diffractometer in Cu-Kα radiation. Microhardness was measured using a Thixomet Smart-Drive microhardness tester; the loads were selected for of each phase. The microstructure of products made from alloys was studied on an MIM-8 microscope. In the microstructure analysis, polished sections etched with a 1:1 mixture of concentrated NaOH and H_2O_2, were examined under a MIM-8 microscope. The density of the alloys was determined by the pycnometric method; toluene was used as filler.

The electrical conductivity of the alloys was measured by the standard compensation method [25] using samples in the form of
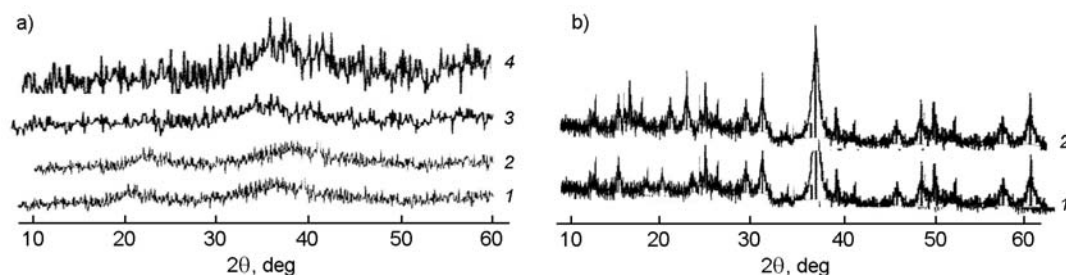
Fig. 1. X-ray powder diffraction patterns of glassy alloys of the As_2Se_3–CdSe system before annealing: *1* — 5; *2* — 15; *3* — 20; *4* — 25 mol. % CdSe (a) and *1* — 5: *2* — 15 mol. % CdSe after annealing (b).
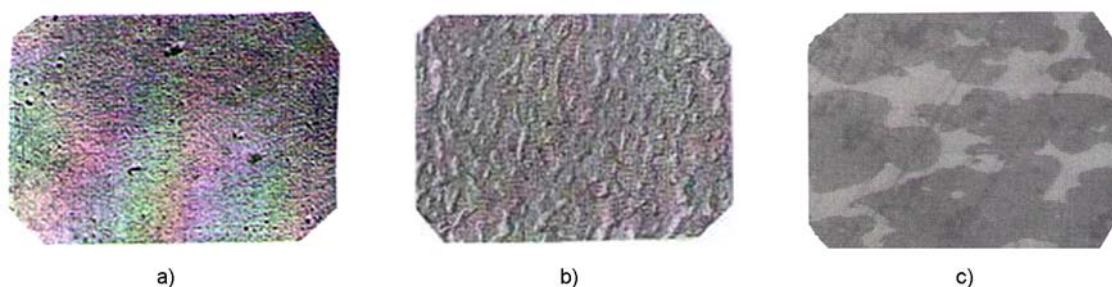

Fig. 2. The microstructure of As_2S_3–CdSe alloys (×340): 10 mol. % CdSe (a — slow cooling, b — cooling in ice water at 623 K); 50 mol. % CdSe (c).

rectangular parallelepipeds. Experimental error was 2.7–3.0 %. The optical properties of the $Cd_3As_2S_3Se_3$ compound were investigated. A nanostructured thin film of the $Cd_3As_2S_3Se_3$ compound was obtained by vacuum deposition. To study the optical properties of the $Cd_3As_2S_3Se_3$ thin film, a U-5100 spectrophotometer was used. The study of photoelectric properties of the alloys was carried out by the methods described in [26].

3. Results and discussion

The alloys of the As_2S_3–CdSe system were obtained in the form of compact and glassy materials and had a red color. All the alloys were stable in air, water and organic solvents and poorly soluble even in mineral acids. Rich CdSe alloys are readily soluble in concentrated mineral acids (HNO_3 and H_2SO_4). Glassy alloys are well soluble in alkalis (NaOH and KOH).

For crystallization, glassy alloys were annealed for 720 h at a temperature of their crystallization (443 K). The alloys of the As_2S_3–CdSe system were investigated before and after annealing. The results of DTA before annealing show the softening temperature T_g on thermograms of alloys in the concentration range of 0–20 mol. % CdSe. After a long annealing (720 h) on the

thermograms of these areas, the softening temperature (443 K) disappears and only the effects related to the liquidus and solidus remain (Tables 1, 2).

Table 1 shows the softening point 443 K for glassy alloys. The microstructure of the As_2S_3–CdSe alloys in the range of 0–20 mol. % CdSe before annealing actually represents one opaque phase.

Glass formation is highly dependent on the chemical nature of atoms, the nature of the electron interaction between the components, and the characteristics of the short-range order in the molten state. A necessary condition for glass formation is the presence of covalent bonds, both in the solid state and in the melt. With an increase in the metallization of the chemical bond, glass formation decreases.

Measurements of the microhardness of cast As_2S_3–CdSe alloys show three different microhardness values in the system (Tables 1, 2). Before and after annealing, the microhardness in the region differs significantly, while the crystal regions remain unchanged. Before annealing, the microhardness of glassy alloys is $H\mu = (1300–1390)$ MPa, density $\rho = (3.20–3.86) \cdot 10^3$ kg/m³. After annealing, the microhardness of the same alloys is $H\mu = (660–690)$ MPa, density $\rho = (3.40–3.90) \cdot 10^3$ kg/m³. To deter-

Table 1. Composition, DTA results, microhardness and density for alloys of As_2S_3–CdSe system (glassy form)

Components, mol. %		Thermal effects, K	Density, $10^3 \cdot kg/m^3$	Microhardness, MPa		
As_2S_3	CdSe			As_2S_3	$Cd_3As_2S_3Se_3$	α
				$P = 0.15$ N		
100	0.0	443.583	3.20	1350	–	–
97	3.0	443.543.578	3.30	1380	–	–
95	5.0	443.543. 573	3.34	1390	–	–
90	10	443.543.568	3.42	1380	–	–
85	15	443.543.558	3.65	1390	–	–
80	20	443.543	3.86	–	–	–
70	30	443.543.623	4.10	–	1170	–
60	40	543.683	4.39	–	1170	–
50	50	543.728	4.63	–	1170	–
45	55	543.728,873	4.71	–	1170	–
40	60	543.728.978	4.77	–	1170	–
30	70	728.978.1133	5.03	–	1170	–
25	75	728.1203	5.15		1170	–
20	80	728.1278	5.25	–	1160	970
10	90	728.1403	5.60	–	1160	970
5.0	95	1073.1468	5.71		–	970
3.0	97	1373.1503	5.76		–	980
0.0	100	1512	5.80		–	950

Table 2. Composition, DTA results, microhardness and density for alloys of As_2S_3–CdSe system (crystalline form)

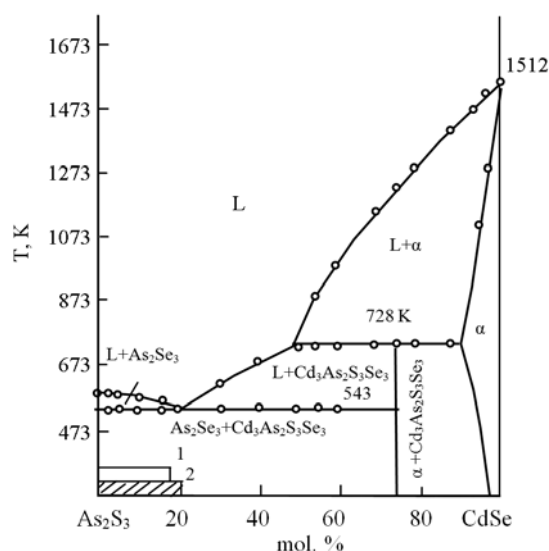| Components, mol. %		Thermal effects, K	Density, $10^3 \cdot kg/m^3$	Microhardness, MPa		
As_2S_3	CdSe			As_2S_3	$Cd_3As_2S_3Se_3$	α
				$P = 0.10$ N		
100	0.0	583	3.46	660	–	–
97	3.0	543.578	3.52	670	–	196
95	5.0	543.573	3.57	690	– –	
90	10	543.568	3.68	690	–	–
85	15	543.558	3.75	690	– –	
80	20	543	3.95	eutectic	eutectic	–
70	30	543.623	4.17	–	–	–
60	40	543.683	4.42	–	1170	–
50	50	543.728	4.63	–	1170	–
45	55	543.728.873	4.72	–	1170	–
40	60	543.728.978	4.77	–	1170	–
30	70	728.978.1133	5.03	–	1170	–
25	75	728.1203	5.15	–	1170	–
20	80	728.1278	5.25	–	1170	970
10	90	728.1403	5.60	–	1170	970
5.0	95	1073.1468	5.73	–	–	970
3.0	97	1373.1503	5.78	–	–	980
0.0	100	1512	5.80	–	–	950

Fig. 3. Phase diagram of the As_2S_3–CdSe system. *1* — glass region at slow cooling, *2* — glass region for quenching in the air.

Fig. 4. Temperature dependences of electrical conductivity for glasses in the As_2S_3–CdSe system: *1* — As_2S_3, *2* — 5, *3* — 10, *4* — 15, *5* — 20, *6* — 25 mol. % CdSe.

mine the region of glass formation in the system, X-ray phase analysis was performed before and after annealing. Before annealing, in alloys with a concentration of 5, 15, 20, and 25 mol.% CdSe, no strong diffraction peaks were found (Fig. 1a). Alloys containing 20 and 25 mol. % CdSe, refer to the glass-crystalline region.

After annealing, strong peaks appear on the diffraction patterns of these alloys (Fig. 1b). This means that 5 and 15 mol. % CdSe glassy alloys after annealing are completely crystallized. The microstructure of the alloys was studied by a microscopic method. The results of the microstructure analysis showed that in the concentration range of 0–30 mol. % CdSe, all the obtained alloys are glassy (Fig. 2). Before annealing, the microstructure of the alloy under a microscope looks like a dark single-phase. To find the new phase and the range of solid solutions, alloys with a concentration of 0–30 mol. % CdSe were annealed at 523 K, and alloys with a concentration of 30–100 mol. % CdSe were annealed at 723 K for 200 h. After the crystallization of the alloys, microscopic analysis was performed; the microstructure of the alloys shows: a) and b) glassy phases; c) two-phase region (Fig. 2).

As a result of the microstructure analysis, a limited region of the solid solution and one new compound of the $Cd_3As_2S_3Se_3$ composition were detected.

Based on the results of physicochemical analysis of the samples, the phase diagram of the As_2S_3–CdSe system (Fig. 3) was con-
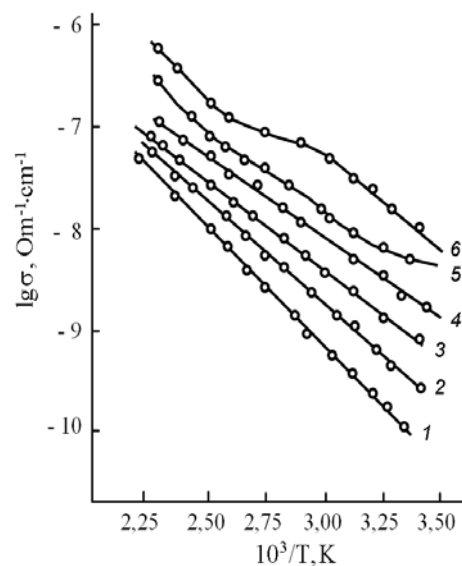
structed. The As_2S_3–CdSe system is a quasi-binary section of the quaternary system As–Cd–S–Se. The $Cd_3As_2S_3Se_3$ compound was obtained with the As_2S_3/CdSe ratio of 1:3. This compound $Cd_3As_2S_3Se_3$ melts incongruently at 728 K.

In the As_2S_3–CdSe system, solid solutions based on CdSe are formed up to 2 mol.% of As_2S_3, and solid solutions based on As_2Se_3 are practically not found. The liquidus of the As_2S_3–CdSe system consists of three phases of primary crystallization: As_2Se_3, $Cd_3As_2S_3Se_3$ and the α-phase (solid solutions based on CdSe). At the concentration interval of 0–75 mol.% CdSe, the two-phase region $(As_2Se_3 + Cd_3As_2S_3Se_3)$ is formed between the liquidus and solidus curves.

Eutectic points of the As_2S_3–CdSe system have coordinates 543 K and 15 mol.% CdSe. In Fig. 3 the microstructures of various alloys of the system are given.

There is a relationship between the glass formation and the character of the phase diagram in the system. This area is located in the concentration range of 0–15 mol.% CdSe. Within the concentration range of 0-20 mol.%, the CdSe structure of the alloys is determined by the structure of As_2S_3 glasses. The crystallization ability of the glasses was investigated as a function of temperature, time and composition.

It is known that crystallization of the glass corresponding to the compound occurs easily in the system, in contrast to the glass
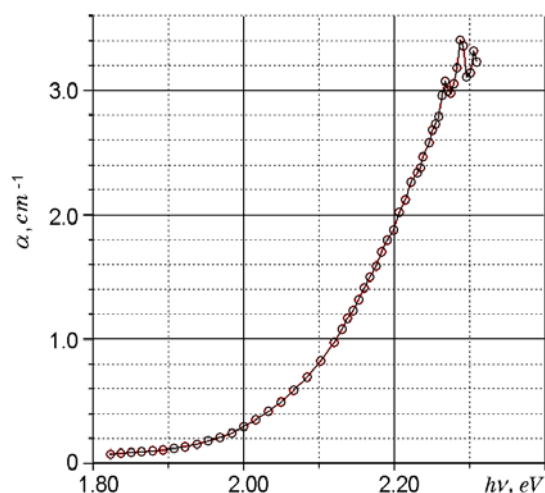
Fig. 5. Absorption spectrum of a thin film of the $Cd_3As_2S_3Se_3$ compound.

Fig. 6. Nanosized thin film of the $Cd_3As_2S_3Se_3$ compound.

Table 3. Interplanar spacings (d, Å), hkl indices, and relative peak intensities in the $Cd_3As_2S_3Se_3$ XRD pattern

Intensity	d_{exp}	d_{calc}	hkl
33	6.1802	6.1780	100
61	4.8425	4.8507	101
54	3.5542	3.5601	040
82	3.2974	3.3041	102
48	3.0880	3.0905	200
7	2.7968	2.7968	050
20	2.7086	2.7116	132
11	2.6733	2.6764	051
39	2.6077	2.6064	003
11	2.3678	2.3735	060
100	2.0602	2.0602	300
70	1.8908	1.8854	024
8	1.7630	1.7658	322
8	1.7398	1.7387	243
7	1.5683	1.5640	005
7	1.4301	1.4319	045
5	1.3824	1.3862	291
4	1.3561	1.3581	450

of the eutectic composition. There is no detailed information in literature about it. This is mainly due to the fact that the temperature of the eutectic composition is very close to the softening point. Therefore, at the slightest deviation of the temperature, glass crystallization does not occur. With the introduction of the second component CdSe into the As_2Se_3 glass, small crystals form and the glass crystallizes easily. The formation of a metal bond adversely affects the formation of glass. The identification of the $Cd_3As_2S_3Se_3$ compound was confirmed by DTA, XRD, density determination, and measurement of microhardness.

It was established that the maxima obtained on diffraction patterns of the $Cd_3As_2S_3Se_3$ compound differ in intensity and interplanar spacing from the initial components. This proves the formation of a new compound $Cd_3As_2S_3Se_3$ in the As_2S_3–CdSe system. By the results of X-ray powder diffraction analysis, it was found that the $Cd_3As_2S_3Se_3$ compound crystallizes in orthorhombic crystal system with unit cell parameters: $a = 0.618$; $b = 1.424$; $c = 0.782$ nm, $Z = 3$, $\rho_{pycn.} = 4.95 \cdot 10^3$ kg/m^3; $\rho_{X-ray} = 5,04 \cdot 10^3$ kg/m^3. The interplanar spacings (d, Å), hkl indices and relative peak intensities in the XRD pattern of the $F_2Cd_3As_2S_3Se_3$ compound are presented in Table 3.

The electrical conductivity of glasses of the As_2S_3–CdSe system was studied in the temperature range 290−450 K (Fig. 4). The samples were parallelepiped-shaped. According to our data, electrical conductivity of As_2S_3 at room temperature is $2 \cdot 10^{-10}$ Om$^{-1} \cdot$m^{-1},

and the band gap is 2.0 eV, which agrees with the literature data. The temperature dependences of the electrical conductivity of alloys containing 5, 10 and 15 mol % CdSe are linear. The alloys containing 20÷25 mol. % CdSe belong to glass-crystalline regions. The temperature dependence of the electrical conductivity of the samples with 5, 10, 15, 20 and 25 mol. % CdSe in the composition shows that the electrical conductivity increases with the addition of the second component; this appears due to an increase in the metallization of the chemical bond. With increasing temperature, the conductivity of the studied glasses increases significantly.
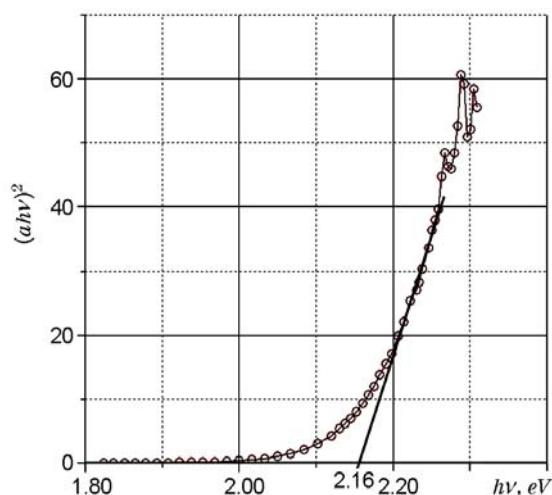
Fig. 7. Photocurrent dependence $(\alpha h\nu)^2$ on $h\nu$ for a thin $Cd_3As_2S_3Se_3$ film.

Fig. 8. Spectral distribution of the photocurrent of the $Cd_3As_2S_3Se_3$ film.

The electrical conductivity results for glasses of the As_2S_3–CdSe system containing 5, 10, 15, 20 and 25 mol.% CdSe in the temperature range 290–450 K are shown in Fig. 4.

Temperature dependence of the electrical conductivity shows that in the As_2S_3–CdSe system, glassy alloys in all temperature ranges have semiconductor conductivity. As can be seen from the graph (Fig. 4), the resistance of alloys containing 5, 10, 15, 20, and 25 % CdSe increases depending on the composition and temperature.

The optical properties of the $Cd_3As_2S_3Se_3$ compound were studied. The nanostructured thin film of the $Cd_3As_2S_3Se_3$ compound was obtained by vacuum deposition. To study the optical properties of a thin film of the $Cd_3As_2S_3Se_3$ compound, a spectrophotometer U-5100 was used.

Fig. 5 shows the absorption spectrum of a thin $Cd_3As_2S_3Se_3$ film. As is known, for the semiconductor state, the direct transition is expressed by the formula [27]

$$\alpha = \frac{1}{h\nu}(h\nu - E_g)^{1/2},$$

where α is the absorption coefficient, $h\nu$ is the energy of a photon, E_g is the semiconductor band gap.

Fig. 6 illustrates nanosized thin films of the $Cd_3As_2S_3Se_3$ compound. To determine the band gap, on the basis of the data obtained, the dependence of $(\alpha h\nu)^2$ versus $h\nu$ for the photocurrent was plotted; and the band gap for the $Cd_3As_2S_3S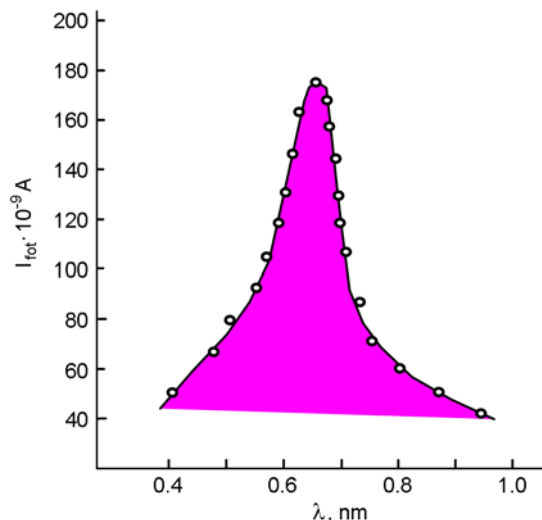e_3$ thin film was determined by linear extrapolation of the linear section to the intersection with the abscissa axis within $E_g = 2.16$ eV (Fig. 7). Fig. 8 shows the spectral distribution of the photocurrent of the $Cd_3As_2S_3Se_3$ compound.

4. Conclusions

The phase diagram of the As_2S_3–CdSe system was plotted. It has been established that the section is a quasibinary cross-section of the quaternary As–Cd–S–Se system. At the ratio of the components 1:3 one quaternary compound of the $Cd_3As_2S_3Se_3$ composition was found in the system, which melts incongruently at 728 K and crystallizes in the rhombic system with the unit cell parameters: $a = 0.618$; $b = 1.424$; $c = 0.782$ nm, $Z = 3$, $\rho_{pycn.} = 4.95 \cdot 10^3$ kg/m^3; $\rho_{X\text{-}ray.} = 5.04 \cdot 10^3$ kg/m^3. The temperature dependence of the electrical conductivity of glassy alloys was studied. The temperature dependence of the electrical conductivity of glassy samples shows that the electrical conductivity increases with the addition of the second component; this is due to an increase in the metallization of the chemical bond. With increasing temperature, the conductivity of the glasses increases significantly. The photoelectric properties of the $Cd_3As_2S_3Se_3$ compound were investigated as a function of the wavelengths of light in the range of 0.4–1 nm. The resulting material can be used as a photo-resistor in optical instruments.

References

1. RF Patent 845685 (1980).

2. P.A.Viktor, V.V.Zotov, V.V.Serdyuk, *FTP*, **13**, 897 (1979).

3. G.A.Kitaev, V.F.Markov, L.N.Maskayeva, *Izv. Acad. Sci. USSR. Inorg. Mater.*, **26**, 248 (1990).

4. N.E.Korsunskaya, I.V.Markevich, A.M.Pavelets et al., *UFJ*, **26**, 1335 (1981).

5. P.Hari, C.Cheneya, G.Luepkea et al., *J. Non-Cryst. Solids*, **270**, 265 (2000).

6. Dinesh Chandra SATI1, Rajendra Kumar, Ram Mohan Mehra, *Turk. J. Phys.*, **30**, 519 (2006).

7. M.S.Iovu, S.D.Shutov, S.Z.Rebeja et al., *J. Optoelectron. Adv. M.*, **2**, 53 (2000).

8. T.Hineva, T.Petkova, C.Popov et al., *J. Optoelectron. Adv. M.*, **9**, 326 (2007).

9. Seema Kandpalm, R.P.S.Kushwaha, *Indian Academy Sci. PRAM ANA J. Phys.*, **69**, 481 (2007).

10. I.C.M.Littler, L.B.Fu, E.C.Magi et al., *Opt. Express*, **4**, 8088, (2006).

11. P.Boolchand, D.G.Georgiev, M.S.Iovu, *Chalc. Lett.*, **2**, 27 (2005).

12. M.S.Iovu, P.Boolchand, D.G.Georgiev, *J. Optoelectron. Adv. M.*, **7**, 763 (2005).

13. T.Kavetskyya, B.Borcs, J.K.Sangwa, *J. Optoelectron. Adv. M.*, **5**, 755 (2011).

14. D.Lezal, J.Zavadil, P.Kostka et al., *J. Non-Cryst. Solids*, **326**, 47 (2003).

15. A.M.Andriesh, V.I.Verlan, *J. Optoelectron. Adv. M.*, **3**, 455 (2001).

16. V.I.Verlan, *J. Optoelectron. Adv. M.*, **5**, 1121 (2003).

17. M.Iovu, S.Shutov, M.Popescu et al., *J. Optoelectron. Adv. M.*, **1**, 15 (1999).

18. Erwan Guillevic, Xianghua Zhang, Jean-Luc Adam et al., *J. Non-Cryst. Solids*, **357**, 2897 (2011).

19. M.Barj, O.A.Mykavlo, D.I.Kaynts et al., *J. Non-Cryst. Solids*, **357**, 2232 (2011).

20. A.V.Stronski, M.Vlcek, A.I.Stetsun et al., *J. Non-Cryst. Solids*, **270**, 129 (2000).

21. P.Hari, C.Cheney, G.Luepke et al., *J. Non-Cryst. Solids*, **270**, 265 (2000).

22. I.I.Aliyev, Doct. Dissertation, Baku (1992).

23. P.G.Rustamov, I.I.Aliyev, *Zh. Neorg. Khimii*, **31**, 771 (1986).

24. I.I.Aliev, B.B.Kuliev, A.P.Gurshumov et al., *Zh. Neorg. Khimii*, **33**, 1618 (1988).

25. A.S.Okhotin, A.S.Pushkarsky, R.P.Borovikova et al., Methods for Measuring the Characteristics of Thermoelectric Materials and Converters, Nauka, Moscow (1974) [in Russian].

26. S.M.Ryvkin. Photoelectric Phenomena in Semiconductors. Fizmatgiz, Moscow (1963) [in Russian].

27. V.I.Gavrilenko, A.M.Grekhov, D.V.Korbutyak et al., Optical Properties of Semiconductors: a Handbook, Naukova Dumka, Kiev (1987).